Available online at www.sciencedirect.com
SCIENCE DIRECT®
Journal of Solid State Chemistry 178 (2005) 135–141
JOURNAL OF SOLID STATE CHEMISTRY
www.elsevier.com/locate/jssc

High-pressure synthesis and X-ray powder structure determination of the nitridophosphate BaP_2N_4

Friedrich W. Karau, Wolfgang Schnick*

Department Chemie und Biochemie, Ludwig-Maximilians-Universität München, Lehrstuhl für Anorganische Festkörperchemier, Butenandtstraße 5-13 (Haus D), D-81377 München, Germany

Received 7 September 2004; received in revised form 27 October 2004; accepted 28 October 2004

Abstract

The novel nitridophosphate BaP_2N_4 was obtained by means of high-pressure high-temperature synthesis utilizing the multianvil technique (8 GPa, 1400 °C). The $[PN_2]^-$ network is isoelectronic with silica. The structure was solved from synchrotron powder data by a combination of direct methods and difference FOURIER synthesis and refined using the RIETVELD method (BaP_2N_4, $Pa\bar{3}$, $Z = 12$, $a = 10.22992(2)$ Å). BaP_2N_4 is isotypic with $BaGa_2S_4$, $BaAl_2S_4$ and the high-pressure phase of CaB_2O_4. The ^{31}P solid-state NMR yielded a single sharp resonance at 0.4 ppm.

Keywords: High-pressure synthesis; Phosphorus nitrides; Crystal structure; Powder diffraction; Solid-state NMR

1. Introduction

In the past decade, we have performed a detailed investigation of several nitridophosphates [1–5]. We have also been able to fully characterize the nitride P_3N_5 [6–8] which is the binary parent compound of all nitridophosphates. Less condensed nitridophosphates with molar ratio $P:N \leqslant 1:2$ usually exhibit PN substructures in analogy with conventional (oxo)silicates or (oxo)phosphates (e.g. HPN_2 (= PN(NH)), $Li_{10}P_4N_{10}$, Ca_2PN_3) [9]. These are obtained by conventional solid-state reactions of the respective binaries. Only a very few nitridophosphates with molar ratio $P:N = 1:2$ have been obtained analogously, e.g. $LiPN_2$, $Zn_7P_{12}N_{24}Cl_2$ [9].

According to our experience, nitridophosphates with molar ratio $P:N > 1:2$ cannot be synthesized by simple reactions of the respective binary starting materials, because the resulting highly condensed PN network structures do not easily crystallize. On the one hand, the reconstructive crystallization of highly condensed PN network structures is not achieved at temperatures below 1000 °C. On the other hand, phosphorus nitride P_3N_5 and most of the nitridophosphates decompose above 850 °C. Therefore, specific synthetic approaches have been developed for the synthesis of highly condensed PN compounds like P_3N_5 [6] or HP_4N_7 (= $P_4N_6(NH)$) [10], which have been obtained by pyrolysis of particular molecular precursor compounds like $P(NH_2)_4I$ or $(NH_2)_2P(S)NP(NH_2)_3$, respectively. Nevertheless, this approach cannot be easily extended to other highly condensed metal nitridophosphates with molar ratio $P:N > 1:2$.

Recently, we achieved the synthesis of novel, highly condensed ternary nitridophosphates by the reaction of the respective metal azides with P_3N_5 utilizing high-pressure reactions (around 3.5 GPa) [1,2]. Typically, these nitridophosphates (e.g. $M^{+I}P_4N_7$ with M^{+I} = Na, K, Rb, Cs; $M^{+I}_3P_6N_{11}$ with M^{+I} = Rb, Cs) have crystal structures deriving from those of isoelectronic alkaline earth (oxo)gallates and (oxo)aluminates.

Now, we are targeting novel metal nitridophosphates with molar ratio $P:N = 1:2$. These compounds are

*Corresponding author. Fax: +49 89 2180 77440.
E-mail address: wolfgang.schnick@uni-muenchen.de (W. Schnick).

0022-4596/$ - see front matter © 2004 Elsevier Inc. All rights reserved.
doi:10.1016/j.jssc.2004.10.034

made up of PN network structures which are isoelectronic with SiO_2. $LiPN_2$ and $Zn_7P_{12}N_{24}Cl_2$ [9], which are obtained by conventional solid-state reactions (see above), already contain SiO_2 analogous $[PN_2]^-$ network structures. Now, we utilized the azide route (see Section 2) for the synthesis of novel nitridophosphates with molar ratio P : N = 1 : 2. The first example is BaP_2N_4, which is described in this contribution.

2. Experimental procedure

As outlined before, increasing the temperature above 850 °C does not activate the desired reconstructive crystallization of nitridophosphates to a long-range ordered and crystalline structure, but it causes an irreversible thermal decomposition under evolution of N_2. Therefore, crystalline and highly condensed phosphorus nitrides were synthesized at both high temperatures (>1000 °C) and high pressures (>5 GPa). To additionally prevent thermal decomposition of the phosphorus nitrides, the nitrogen partial pressure was increased by in situ decomposition of a metal azide according to Eq. (1). During this reaction the metal azide is transformed into the respective metal nitride which immediately reacts with the phosphorus nitride under formation of the desired product according to Eq. (2) (the so-called azide route).

$$3\,Ba(N_3)_2 \xrightarrow[>3.5\,GPa]{>1000\,^\circ C} Ba_3N_2 + 8N_2, \quad (1)$$

$$2\,P_3N_5 + 3\,Ba(N_3)_2 \xrightarrow[8\,GPa]{1400\,^\circ C} 3\,BaP_2N_4 + 8\,N_2. \quad (2)$$

The high-pressure reactions were performed utilizing the multianvil technique and a WALKER-type module. Under these conditions the reaction temperature could be increased up to 1500 °C without decomposition of the phosphorus nitrides. Details of the experimental setup are given in [7].

As starting materials for the high-pressure high-temperature synthesis of BaP_2N_4 we used P_3N_5 and $Ba(N_3)_2$. These compounds were synthesized starting from commercial hexachlorocyclotriphosphazene (Merck, p.a.) and gaseous ammonia (Messer Griesheim, 3.8) as well as barium hydroxide (Merck, p.a.).

2.1. Synthesis of phosphorus(V) nitride

Phosphorus(V) nitride was obtained by the reaction of gaseous ammonia with hexachlorocyclotriphosphazene in accordance with [11]. The reaction was carried out at 950 °C in a gas flow of dried ammonia (dried by flowing through a column (l = 1000 mm, ∅ = 50 mm) filled with KOH pellets).

2.2. Synthesis of barium azide

Barium azide was obtained by the reaction of barium hydroxide with an aqueous solution of HN_3, synthesized from NaN_3 (Merck, p.a.) and H_2SO_4 by destillation, in accordance with [12]. $Ba(N_3)_2$ was dried over P_4O_{10} using a vacuum desiccator.

2.3. Synthesis of BaP_2N_4

The high-pressure synthesis of BaP_2N_4 was carried out using the multianvil technique and a hydraulic press [13,14] according to Eq. (2). Cr_2O_3-doped MgO octahedra (Ceramic Substrates & Components Ltd, Isle of Wight) with an edge length of 18 mm were used. Eight truncated tungsten carbide cubes separated by pyrophyllite gaskets served as anvils for the compression of the octahedra. The truncation edge length was 11 mm.

A mixture of barium azide and partially crystalline phosphorus(V) nitride, prepared as described in section 2.1, was ground thoroughly and loaded into a cylindrical capsule of hexagonal boron nitride (Henze, Kempten) with a capacity of 35 mm^2 and sealed with a BN cap. The capsule was centered within two nested graphite tubes, which acted as an electrical resistance furnace. The remaining volume and both ends of the sample capsule were filled out with two cylindrical pieces of magnesium oxide. The arrangement was placed into a zirconium dioxide tube and then transferred into a pierced MgO octahedron. The electrical contact of the graphite tubes was arranged by two plates of molybdenum.

The assembly was compressed up to 8 GPa at room temperature within 3.5 h and then heated up to 1400 °C within 25 min. Under these conditions the sample was treated for 40 min and finally cooled down to room temperature during 1 h. Subsequently, the pressure was released within a period of 8 h. After the reaction was completed, about 95 mg BaP_2N_4 were obtained as a colorless and crystalline powder.

The temperature was calculated from the electrical power applied to the furnace which was determined on the basis of calibration curves from measurements with $W_{97}Re_3$–$W_{75}Re_{25}$ thermocouples, as described in [14,15].

2.4. Solid-state NMR investigation

The ^{31}P MAS NMR spectrum (Fig. 1) was acquired with a rotation frequency of ν_{rot} = 15 kHz using a conventional FOURIER-transform NMR spectrometer DSX Avance (Bruker, Germany) working with a resonance frequency ν_0 = 202.5 MHz for the ^{31}P nuclei. The data collection was carried out with a single pulse sequence and a repetition delay of 200 s to guarantee complete relaxation. The 90° pulse length was adjusted

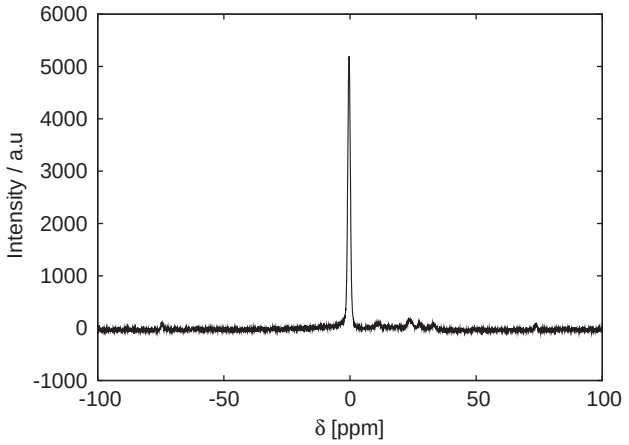

Fig. 1. ^{31}P MAS NMR spectrum of BaP_2N_4.

to 2.1 μs. The spectrum is referenced according to phosphoric acid (85%).

2.5. X-Ray powder diffraction

Initially the powder diffraction pattern collected on a Stoe StadiP diffractometer (Stoe &Cie, Darmstadt) using Mo$K\alpha$1 radiation could not be indexed unambiguously. This shortcoming resulted from the presence of an unknown and uncharacterized minor phase, which could only be discovered using synchrotron radiation (Swiss Norwegian Beamline, Grenoble, histogram see Fig. 2). The title compound and the minor phase show significant differences in the half-widths of the neighboring main diffraction peaks (BaP_2N_4: 0.0237(3)° at 14.88174(8)° (see Fig. 3(a)), minor phase 0.045(2)° at 14.4056(5)° see Fig. 3(b)). Selecting only the reflections of BaP_2N_4, an indexation was successful with the program WERNER [16] (DE-WOLFF figure of merite $M(20) = 90$, $M(30) = 83$, $M(62) = 43$), implemented into the program package CMPR [17]. The lattice is cubic primitive with a lattice parameter of 10.23 Å. Fig. 2(b) shows the resolved diffraction peaks of both the minor phase and BaP_2N_4. According to the observed extinction conditions $0kl$, $h0l$, $hk0$ and $00l$, the space group $Pa\bar{3}$ unequivocally was derived.[1] The space group $Pn\bar{3}$ could be excluded because of the presence of the unambiguous indexed reflection (210). The structure solution and refinement was only possible using space group $Pa\bar{3}$.

The structure was solved on the basis of the integrated intensities from a LE BAIL fit performed in the space group $Pa\bar{3}$ with the program GSAS [18] implemented into the program package EXPGUI [19]. A file containing the MILLER indices and integrated intensities was obtained using the routine *refcalc* implemented into GSAS and converted into a *hklf 4* file readable by SHELX-97 [20] using a data conversion routine written in FORTRAN. The Ba and P atoms were found using SHELXS by direct methods. The nitrogen atoms were located from the difference FOURIER map and added step-by-step during the refinement procedure. The crystallographic data are summarized in Table 1.

The profile fit was performed utilizing a pseudoVOIGT function [21] with asymmetry correction [22]. The anisotropic displacement factor has the form $\exp(-2\pi^2[(ha^\star)^2U_{11} + \cdots + (lc^\star)^2U_{33} + 2U_{23}klb^\star c^\star + 2U_{13}hla^\star c^\star + 2U_{12}hka^\star b^\star)])$. U_{eq} is defined as one-third of the trace of the U_{ij} tensor.

Later on the preparation of phase-pure BaP_2N_4 was successful. Further details of the crystal structure analysis may be obtained from the Fachinformationszentrum Karlsruhe, D-76344 Eggenstein-Leopoldshafen, Germany, by quoting the depository number CSD-414350.

The crystallographic results are consistent with the ^{31}P-NMR spectrum (Fig. 1). The spectrum shows one ^{31}P signal at 0.4 ppm corresponding with one crystallographic phosphorus site (see Table 2). The observed chemical shift is in the same region (−23.5 ppm (NaP_4N_7) to 54.6 ppm (Li_7PN_4)) as those of other ternary nitridophosphates. An overview is given in [25]. Likewise it agrees with the shift of other nitridophosphates with a molar ratio P : N = 1 : 2, e.g. $LiPN_2$ [23] with a shift of 0 ppm.

The thermal stability of BaP_2N_4 at ambient pressure was investigated by temperature programmed powder diffraction on a Stoe StadiP diffractometer with mounted electrical furnace using Mo$K\alpha$1 radiation. Surprisingly, neither a phase transition nor decomposition occurred up to 1050 °C in air. After about 10 min at 1100 °C, amorphization was observed. Accordingly, cubic BaP_2N_4 does not seem to be a *classical* high-pressure phase, which would show a thermally induced first order, irreversible phase transition. Furthermore, the chemical stability of BaP_2N_4 against air at high temperatures significantly exceeds that of the binary parent compound P_3N_5, which decomposes above 850 °C in argon atmosphere.

3. Description of the structure

The result of the crystal structure refinement with the RIETVELD method based on the synchrotron data is shown in Table 2. Within the accuracy of the measurement these data agree well with those obtained from phase pure material utilizing Mo$K\alpha$1 radiation (Table 3). Selected interatomic bond distances and bond angles are given in Tables 4 and 5.

[1] For the extinction condition $0kl$, $h0l$ and $hk0$ only cyclic permutations are permitted.

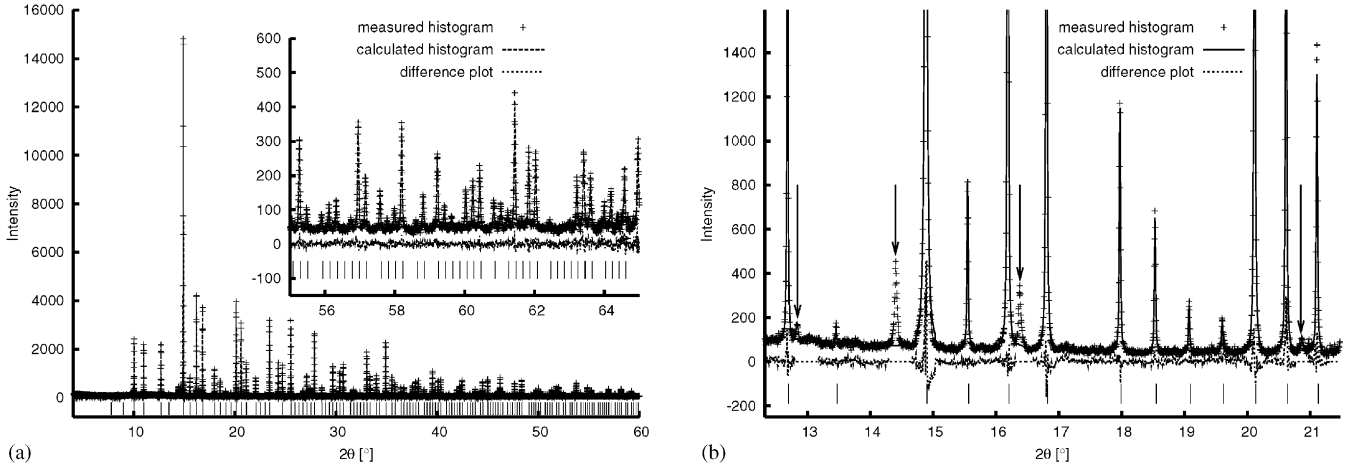

Fig. 2. The synchrotron measurement resolves the diffraction pattern of BaP_2N_4 and the unknown minor phase completely. The inset shows the good signal-to-noise ratio at high angles. (a) Whole diffraction pattern of BaP_2N_4 and (b) Histogram of BaP_2N_4 and minor phase (marked with an arrow).

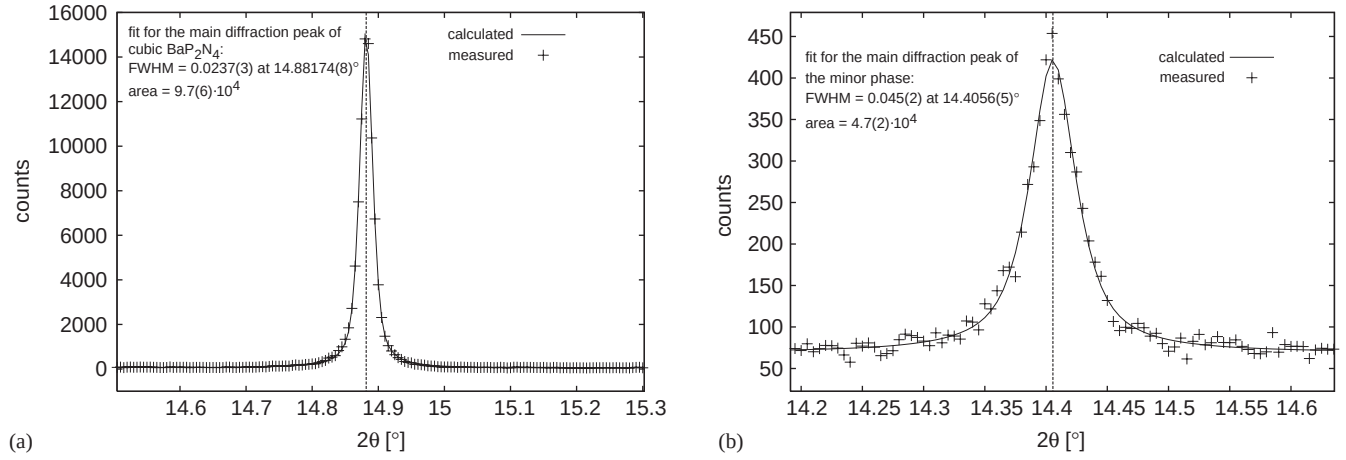

Fig. 3. Fitted main diffraction peaks and calculated half-width of cubic BaP_2N_4 (a) and the unknown minor phase (b) taken from the synchrotron measurement.

The crystal structure of BaP_2N_4 (see Fig. 4) is isotypic with that of $BaGa_2S_4$, $BaAl_2S_4$ [27] and HP-CaB_2O_4 [28]. In the crystal there are Ba^{2+} ions embedded into a framework structure of corner sharing PN_4 tetrahedra (see Fig. 5). From a formula point of view, the $[P_2N_4]^{2-}$ substructure is isoelectronic with SiO_2. Nevertheless, its topology is rather different to any known SiO_2 polymorph. $[P_3N_3]$ 3-rings (see Fig. 6(a)) occur as fundamental building units. These 3-rings are exclusively made up of P(1) and N(1). The distances P(1)–N(1) amounts to 1.630(6) and 1.658(6) Å, respectively (Tables 4 and 5). N(2) connects the 3-ring units with other 3-ring units. The distance P(1)–N(2) is 1.661(7) Å and 1.633(6) Å, respectively. These values are similar to the P–N distances determined for HPN_2 [29] and $LiPN_2$ [24] (1.599(4) and 1.645(7) Å). Accordingly, each 3-ring unit is connected to six other neighboring units. The resulting framework thus contains 6- and 7-rings (see Fig. 6). The N–P–N angles are between 105.1(3) and 112.5(4) varying around the respective angles in HPN_2 [29] and $LiPN_2$ [24] (107.5(5)–113.4(5), 107.0(5)–114.5(2)°). The P(1)–N(1)–P(1) angle of BaP_2N_4 is 121.7(4) and the P(1)–N(2)–P(1) angle is 125.3(4)° according to the respective P–N–P angles in HPN_2 [29] (130.1(4)°) and $LiPN_2$ [24] (123.6(8)°). The cycle class sequence (i.e. the relative frequency of the P_nN_n ring sizes occurring in the network for $n = 1, 2, 3, \ldots$) has been calculated with the program TOPOLAN [30] and it amounts to $\{-, 0, 8, 0, 0, 4, 24, 72, \ldots\}$.

Table 1
Crystallographic data for BaP_2N_4, for the synchrotron and the diffractometer (Stoe StadiP) measurement

	Synchrotron	Stoe StadiP
Crystal data		
Formula units	12	
Chemical formula	BaP_2N_4	
Crystal system, space group	Cubic, $Pa\bar{3}$ (No. 205)	
Unit cell dimensions (Å)	$a = 10.22992(2)$	$a = 10.2200(2)$
Cell volume (Å^3)	1070.575(3)	1067.46(2)
X-ray density, ρ (g cm^{-3})	4.752	4.766
Data collection		
Radiation	Synchrotron	Mo$K\alpha$1
Wavelength λ (Å)	0.7996002	0.70930
Observed reflections	$N_{obs} = 465$	$N_{obs} = 546$
Measured data points	12 292	5242
2Θ-range	$4.03 \leqslant 2\Theta \leqslant 65.485$	$7.0 \leqslant 2\Theta \leqslant 59.98$
Step size (°)	0.005	0.01
Refinement with GSAS		
Background function	Chebyshev-function	
Background points	44	32
Profile function	Pseudovoigt funct. with asym. corr.	
Excluded regions2Θ(°)	[9.1450, 9.7950] [11.330, 12.350] [12.790, 13.170] [14.290, 14.630] [16.310, 16.590] [20.770, 20.975] [21.310, 21.955] [23.685, 24.045] [32.165, 32.300] [33.490, 33.785]	No excluded regions
R-values	$R(F^2) = 0.053$ wRp_{fit} = 0.117 $Rp_{fit} = 0.093$ w$Rp_{back} = 0.082$ $Rp_{back} = 0.074$	$R(F^2) = 0.063$ w$Rp_{fit} = 0.080$ $Rp_{fit} = 0.061$ w$Rp_{back} = 0.080$ $Rp_{back} = 0.063$

Table 2
Atomic coordinates anisotropic and isotropic displacement parameters (multiplied by 100) of BaP_2N_4 (synchrotron measurement)

Atom	*x*	*y*	*z*	$U_{iso/eq}$	U_{11}	U_{22}	U_{33}	U_{12}	U_{13}	U_{23}
Ba(1)	0	0	0	1.09(2)	1.09(2)	U_{11}	U_{11}	−0.27(4)	U_{12}	U_{12}
Ba(2)	0.36863(5)	*x*	*x*	0.35(1)	0.35(1)	U_{11}	U_{11}	0.00(2)	U_{12}	U_{12}
P(1)	0.1861(2)	0.3342(2)	0.1088(2)	0.30(4)	0.30(4)	U_{11}	U_{11}	0	0	0
N(1)	0.3225(6)	0.2520(6)	0.1112(6)	0.08(9)	0.08(9)	U_{11}	U_{11}	0	0	0
N(2)	0.2205(6)	0.4920(7)	0.0920(6)	0.08(9)	0.08(9)	U_{11}	U_{11}	0	0	0

The displacement parameters of N(1) and N(2) are set to be equal.

Table 3
Atomic coordinates anisotropic and isotropic displacement parameters (multiplied by 100) of BaP_2N_4 (Mo$K\alpha$1-diffractometer)

Atom	*x*	*y*	*z*	$U_{iso/eq}$	U_{11}	U_{22}	U_{33}	U_{12}	U_{13}	U_{23}
Ba(1)	0	0	0	1.85(3)	1.85(3)	U_{11}	U_{11}	−0.46(6)	U_{12}	U_{12}
Ba(2)	0.36858(9)	*x*	*x*	1.17(2)	1.17(2)	U_{11}	U_{11}	−0.14(4)	U_{12}	U_{12}
P(1)	0.1850(4)	0.3341(4)	0.1083(3)	1.25(8)	1.25(8)	U_{11}	U_{11}	0	0	0
N(1)	0.3216(7)	0.2508(8)	0.1062(9)	0.5(2)	0.5(2)	U_{11}	U_{11}	0	0	0
N(2)	0.2181(8)	0.490(1)	0.0979(9)	0.5(2)	0.5(2)	U_{11}	U_{11}	0	0	0

The displacement parameters of N(1) and N(2) are set to be equal.

Table 4
Selected bond distances in Å and bond angles in °

Atom	Synchrotron	Mo$K\alpha$1-Diffrac.
P(1)–N(1)	1.630(6)	1.635(8)
	1.658(6)	1.669(8)
P(1)–N(2)	1.661(7)	1.63(1)
	1.633(6)	1.60(1)
P(1)–N(1)–P(1)	121.7(4)	120.9(6)
P(1)–N(2)–P(1)	125.3(4)	129.4(5)

Table 5
N–P–N angles in °

Atom	Synchrotron	Mo$K\alpha$1-Diffrac.
N(1)–P(1)–N(1)	110.2(4)	112.5(6)
N(1)–P(1)–N(2)	108.7(4)	109.3(5)
N(1)–P(1)–N(2)	109.8(3)	107.0(5)
N(1)–P(1)–N(2)	105.1(3)	103.4(4)
N(1)–P(1)–N(2)	110.5(3)	111.5(5)
N(2)–P(1)–N(2)	112.5(4)	113.2(6)

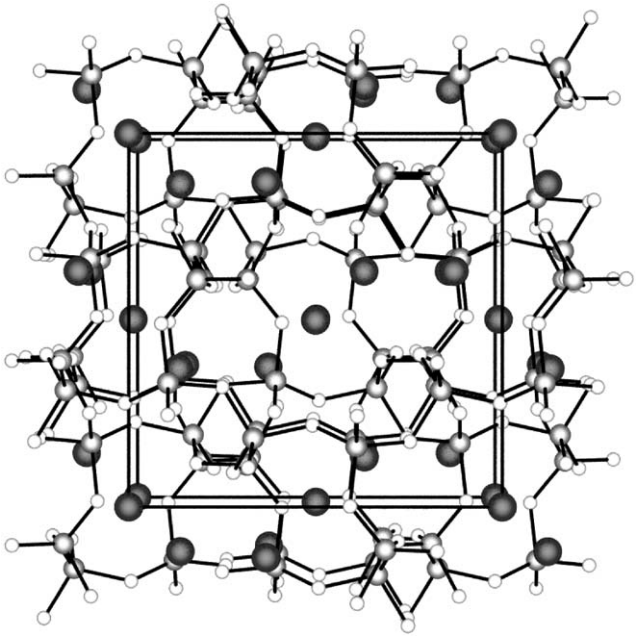

Fig. 4. Crystal structure of BaP_2N_4, view along [001].

This arrangement of PN_4 tetrahedra forms large empty cages in which the Ba^{2+} ions are situated. The Ba(1)–N distances are 3.320(6) (Ba(1)–N(1)) and 3.011(6) Å (Ba(1)–N(2)). The Ba(2)–N distances are between 2.811(6) (Ba(2)–N(1)) and 3.449(6) Å (Ba(2)–N(2)). These distances roughly correspond with the sum of the ionic radii [31]. Both Ba^{2+} ions are 12-fold coordinated.

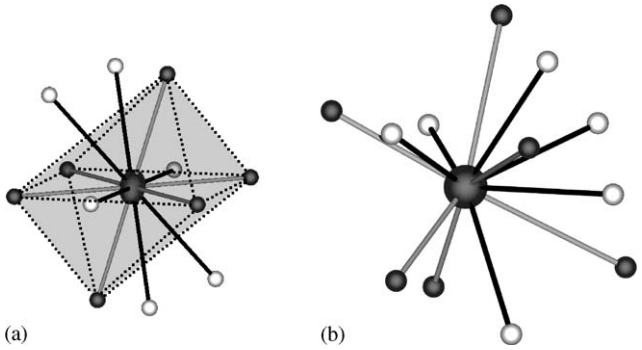

Fig. 5. Ba(1) is connected to six N(1) (gray) and N(2) (black) with distances 3.320(6) and 3.011(6) Å. The coordination of Ba(1) with N(2) is a significant distorted octahedron. Ba(2) is also connected to six N(1) and six N(2) with distances between 2.811(6) and 3.449(6) Å. Therefore both Ba atoms have a $6+6$ coordination sphere. (a) Coordination sphere of Ba(1) and (b) coordination sphere of Ba(2).

4. Conclusion

In this contribution the first alkaline earth nitridophosphate with molar ratio $P : N = 1 : 2$, namely BaP_2N_4, is described. It was synthesized by means of high-pressure high-temperature synthesis and characterized by synchrotron powder diffraction and MAS solid state NMR. Whereas the parent compound P_3N_5 decomposes above 850 °C, BaP_2N_4 is stable up to 1050 °C in air.

While other nitridophosphates with molar ratio $P : N = 1 : 2$ (e.g. HPN_2 [29], $LiPN_2$ [24] and $NaPN_2$ [26]) show structural similarities to silica analogous networks BaP_2N_4 forms a PN_4 tetrahedral network, that shows similarities to thiogallates and thioaluminates. Currently, we are expanding our focus on $M^{+II}P_2N_4$ compounds of alkaline earth elements or other bivalent metals, which have SiO_2 isoelectronic $[PN_2]^-$ networks. Especially we are investigating the compounds $M^{+II}P_2N_4$, with $M = Be, Mg, Ca, Sr$. For BeP_2N_4 we expect the transition from an alkaline earth cation containing $[PN_2]^-$ network (*nitridophosphate*) to a *double nitride*, that is completely built up of M^{+II} tetrahedra and P^{+V} tetrahedra. These investigations will be presented in forthcoming papers.

Acknowledgements

The research of W. Schnick was generously supported by the Deutsche Forschungsgemeinschaft and the Fonds der Chemischen Industrie. The authors thank Dr. J. Senker for the NMR investigation.

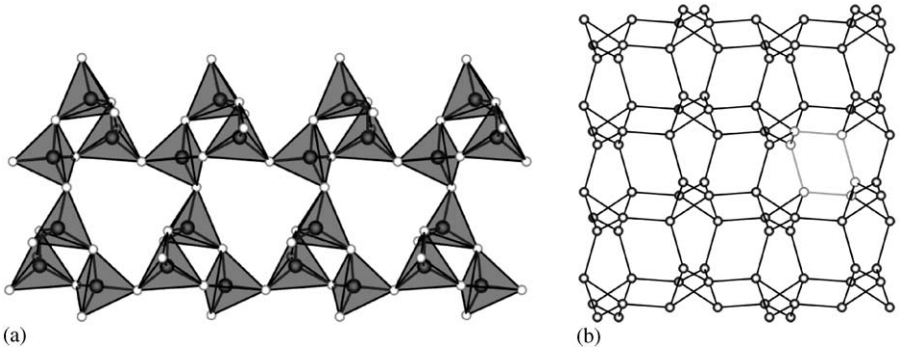

Fig. 6. The left figure is a section of the BaP_2N_4 structure. It shows characteristic 3-rings connected by corner sharing tetrahedra forming 7-rings (view along [001], Ba atoms are left out). The right figure shows the 6-rings (view along [010]). For reasons of clarity only the P-atoms are shown. One 6-ring is marked light gray. (a) 3-rings and 7-rings and (b) 6-rings.

References

[1] K. Landskron, E. Irran, W. Schnick, Chem. Eur. J. 5 (1999) 2548.
[2] K. Landskron, W. Schnick, J. Solid State Chem. 156 (2001) 390.
[3] W. Schnick, J. Lücke, Z. Anorg. Allg. Chem. 620 (1994) 2014.
[4] W. Schnick, N. Stock, J. Lücke, M. Volkmann, M. Jansen, Z. Anorg. Allg. Chem. 621 (1995) 987.
[5] F. Wester, W. Schnick, Z. Anorg. Allg. Chem. 622 (1996) 1281.
[6] S. Horstmann, E. Irran, W. Schnick, Angew. Chem.—Int. Ed. Engl. 36 (1997) 1873.
[7] K. Landskron, H. Huppertz, J. Senker, W. Schnick, Angew. Chem.—Int. Ed. 40 (2001) 2643.
[8] P. Kroll, W. Schnick, Chem. Eur. J. 8 (2002) 3530.
[9] W. Schnick, Angew. Chem.—Int. Ed. Engl. 32 (1993) 806.
[10] S. Horstmann, E. Irran, W. Schnick, Angew. Chem.—Int. Ed. Engl. 36 (1997) 1992.
[11] V. Schultz-Coulon, W. Schnick, Z. Anorg. Allg. Chem. 69 (1997) 623.
[12] G. Brauer, Handbuch der Präparativen Anorganischen Chemie, Ferdinand Enke Verlag, Stuttgart, 3. Auflage, 1978, S. 930.
[13] [a] D. Walker, M.A. Carpenter, C.M. Hitch, Am. Mineral. 75 (1990) 1020;
[b] D. Walker, Am. Mineral. 76 (1991) 1092.
[14] H. Huppertz, Z. Kristallogr. 219 (2004) 330.
[15] D.C. Rubie, Phase Transitions 68 (1999) 431.
[16] P.-E. Werner, Z. Kristallogr. 120 (1964) 375.
[17] B.H. Toby, Program CMPR, Brian.Toby@nist.gov.
[18] A.C. Larson, R.B. von Dreele, Los Alamos National Laboratory Report LAUR, vol. 86, 2000, p. 768.
[19] B.H. Toby, J. Appl. Crystallogr. 34 (2001) 210.
[20] G.M. Sheldrick, SHELX97, Program package for the solution and refinement of crystal structures, Release 97-2 University of Göttingen, Germany, 1997.
[21] P. Thompson, D.E. Cox, J.B. Hastings, J. Appl. Crystallogr. 20 (1987) 79.
[22] L.W. Finger, D.E. Cox, A.P. Jephcoat, J. Appl. Crystallogr. 27 (1994) 89.
[23] H.P. Baldus, W. Schnick, J. Lücke, U. Wannagat, G. Bogedain, Chem. Mater. 5 (1993) 845.
[24] W. Schnick, J. Lücke, Z. Anorg. Allg. Chem. 588 (1990) 19.
[25] K. Landskron, Doctoral Thesis, University of Munich, 2001.
[26] K. Landskron, S. Schmid, W. Schnick, Z. Anorg. Allg. Chem. 627 (2001) 2469.
[27] B. Eisenmann, M. Jakowski, H. Schäfer, Mater. Res. Bull. 17 (1982) 1169.
[28] M. Marezio, J.P. Remeika, D.D. Dernier, Acta Crystallogr. B 25 (1969) 965.
[29] W. Schnick, J. Lücke, Z. Anorg. Allg. Chem. 610 (1992) 121.
[30] G. Thimm, S. Schumacher, W. Uhr, W.E. Klee, TOPOLAN, Topological analysis of crystal structures, Institut für Kristallographie der Universität Karlsruhe, Germany, 2001.
[31] W.H. Baur, Crystallogr. Rev. 1 (1987) 59.